Effect of accelerating electrode rotation on ion beam optics

Elizabeth Surrey

Citation: Rev. Sci. Instrum. **74**, 3329 (2003); doi: 10.1063/1.1578153
View online: http://dx.doi.org/10.1063/1.1578153
View Table of Contents: http://rsi.aip.org/resource/1/RSINAK/v74/i7
Published by the American Institute of Physics.

Effect of accelerating electrode rotation on ion beam optics

Elizabeth Surrey[a)]
UKAEA/EURATOM Fusion Association, Culham Science Centre, Abingdon, Oxfordshire OX14 3DB, United Kingdom

(Received 7 October 2002; accepted 26 March 2003)

The effect of a rotation of the electrode used to accelerate a positive ion beam is treated analytically for the Joint European Torus (JET) Positive Ion Neutral Injector (PINI) tetrode accelerator. The rotation is taken to be about an axis in the plane of the electrode and perpendicular to the beam axis, so the effect is that of a tilt in the alignment of the affected electrode. The effect of such a tilt in either of the two multiaperture accelerating electrodes is to introduce an additional steering of the beam, the magnitude of which depends upon the ratio of the potentials across the first and second accelerating gaps and the position of the beamlet with respect to the tilt axis. The direction of the steering is dependent upon which electrode is displaced. Steering angles of the order 10 mrad can be generated by this effect, which is significant compared to the alignment precision required from high power neutral injectors such as those on JET. The presence of a grid rotation also affects the total perveance of a multiaperture system and this can be used to obtain information on the position of the tilt axis. Typical values are calculated for the JET PINI geometry and compared to observation. [DOI: 10.1063/1.1578153]

I. INTRODUCTION

The steering effect of aperture displacements on the optics of ion beams has long been recognized as a useful aid to controlling the gross beam steering of multiaperture accelerator systems.[1,2] The Joint European Torus (JET) positive ion neutral injector (PINI)[3] exploits this effect to produce a gross beam with focal lengths 14 m (vertical plane) and 10 m (horizontal plane) from 262 individual beamlets. The accelerating electrodes of the PINI are divided into two halves, each inclined at an angle of 8.3 mrad toward the beam axis. Each half electrode contains 131 apertures arranged in a rectangular grid of dimensions 165 mm horizontally by 204 mm vertically (dimensions are taken between the centers of the extreme apertures in the first electrode). Additional steering of each beamlet is introduced at the third electrode by the introduction of an aperture offset varying from zero along the vertical center line of the grid half to 0.16 mm vertically and 0.21 mm horizontally, giving a steering constant of 40 mrad/mm. Note that the aforementioned values pertain to the standard (80 kV/60 A extracted) tetrode PINI only; the values are slightly different for the standard (140 kV/30 A) triode (steering constant 14 mrad/mm), and the upgrade tetrode (21 mrad/mm).[4]

The effect of offset aperture steering has been studied extensively both analytically[2,5] and computationally,[6,7] but only for the case where the electrodes are essentially parallel surfaces. In this treatment, the effect of introducing a rotation of one electrode relative to the others is considered. Specifically, the rotation is assumed to be about an axis perpendicular to the beam axis but within the plane of the electrode, such that one grid is tilted with respect to the general geometry; the analysis applies equally to horizontal and vertical rotations. The motivation for this study was the observation of poor beam optics and an anomalous perveance match condition in one particular tetrode PINI during tests on the neutral beam test bed facility at JET.[4] A subsequent measurement of the positions of each grid half using the FARO-Arm® (FARO Technologies Inc.) three-dimensional coordinate measuring facility at JET[8] revealed that displacements of the second and third electrodes had occurred after the original assembly. Furthermore, upon dismantling the injector, the considerable beam strike was noted on the front of the third electrode, particularly in the lower grid half, where the beamlets had been displaced to the left-hand side when viewed from the ion source. The horizontal movement of the second grid revealed by the FARO-Arm® should have resulted in the beamlets being steered to the right-hand side, thus the simple offset due to misalignment could not explain the observations. An analytical model, based upon the linear optics method of Holmes and Thompson,[9] was derived to investigate the effect of a grid rotation and is described in Sec. II with some results pertinent to the JET PINI given in Sec. III.

II. ANALYTICAL MODEL OF THE ROTATED ELECTRODE

The analytical description of beam steering due to a rotated electrode uses a matrix formulation to calculate particle trajectories at a given radial position within the beam using the paraxial ray equation.[9] The model includes the effect of space charge on the electric fields and the focusing effect caused by the postacceleration of the extracted ions in the second gap.[10] We will consider each accelerating electrode (second and third grids) separately within a tetrode geometry.

[a)]Electronic mail: esurrey@jet.uk

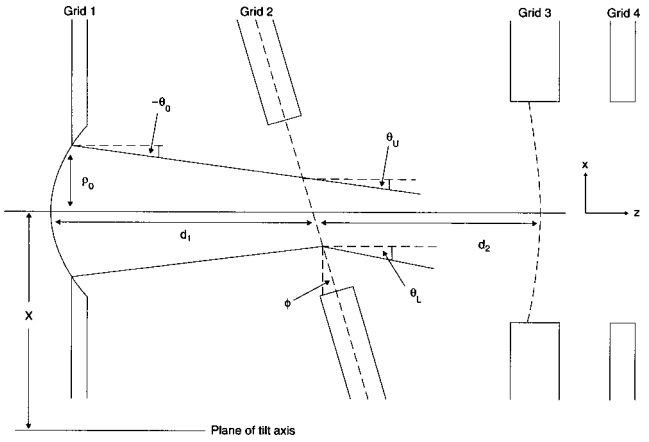

FIG. 1. Geometry for the case of tilted grid 2 in a tetrode accelerator. The electrodes are labeled sequentially from the left- and to the right-hand side.

A. Rotation at the second grid

Figure 1 shows a general grid geometry. Grid 1 is the extraction grid at which the beam is formed from a plasma meniscus. Grid 2 is an accelerating electrode, grid 3 is a decelerating (negative voltage) electrode, and grid 4 is at ground potential. In Fig. 1, the case where grid 2 is tilted in the vertical plane through an angle ϕ with respect to grids 1 and 3 is shown. The case of a tilt in the horizontal plane is identical with the upper portion corresponding to the left-hand side portion of the grid when viewed from the plasma source. The heavy solid lines represent the envelope of the beamlet under consideration. We will adopt the sign convention that an envelope angle toward the axis (in the direction of increasing z) is negative when x is positive and vice versa; the angle ϕ is positive as shown. The cause of the steering is apparent from Fig. 1. Clearly, the gap lengths on either side of grid 2 vary across the beam, giving a gradient in focal length of the lens so that one side of the beam will be deflected through a greater angle. The angle of any given trajectory after passing through the lens is simply:

$$\theta_i = \theta_0 - \frac{x_i}{f_i}, \tag{1}$$

where x_i is the distance from the axis to the trajectory at the second grid and f_i is the local value for the focal length of the lens at x_i. The total steering angle due to the grid tilt is the average of the θ_i values at the edges of the beam in the upper and lower halves of the geometry, viz,

$$\theta_s = \frac{\theta_U + \theta_L}{2}, \tag{2}$$

where the subscripts U and L denote upper and lower parts of the aperture. (NB: In the upper half, x is positive and θ is negative, while in the lower half x is negative and θ is positive. For a rotation in the horizontal plane, x is positive to the left-hand side of the aperture when viewed from the plasma source). The focal length of the lens at grid 2 is given by[9]

$$\frac{1}{f_1} = \frac{\Gamma}{4d_2} - \frac{(1-0.2k)}{3d_1} + \frac{d_2}{9d_1^2}\left[\frac{2}{\Gamma} - \frac{4(U^{1.5}-1)}{3\Gamma^2}\right] \times (1-0.4k), \tag{3}$$

where $\Gamma = V_2/V_1$, the ratio of the potential differences either side of the grid, $U=(\Gamma+1)$ and d_1 and d_2 are the gap lengths on either side of the grid. (In reality, there is a small correction to be made to d_1 and d_2 to account for the curvature of the equipotential surface at grid 2; this will be discussed later).

The parameter k describes the curvature of the plasma boundary and is given by[9] $k = d_1 \sin\theta_0/\rho_0$. Holmes and Thompson[9] further show that the beam perveance, P, is related to the plain diode perveance, P_D, by

$$P = P_D(1+0.8k)^2, \tag{4}$$

to within a 2% error for the range $-0.5 < k < +0.5$. The plain diode perveance is given by

$$P_D = \frac{4\pi\rho_0^2\varepsilon_0}{9d^2}\sqrt{\frac{2e}{m}}, \tag{5}$$

where for a tetrode, $d = d_1 + d_2$.

For a generalized equation, we assume that the aperture is situated a distance X from the tilt axis so that the position due to the tilt is given by

$$X_U = X\cos\phi \approx X, \tag{6}$$

if ϕ is small.

Considering the upper half of the geometry, Eq. (3) can be modified to include the effect of the change in d_1 and d_2 due to the grid tilt. The corrected values d_{1U} and d_{2U} are given by

$$d_{1U} = d_1 - (x_U + X)\phi,$$
$$d_{2U} = d_2 - (x_U + X)\phi. \tag{7}$$

The vertical extent of the beamlet in the upper half of the aperture at grid 2 is given by

$$x_U = \rho_0 + d_{1U}\theta_0. \tag{8}$$

Thus,

$$x_U = \frac{\rho_0 + d_1\theta_0 - X\phi\theta_0}{(1+\theta_0\phi)} = x - \phi\theta_0(x+X), \tag{9}$$

where x is the vertical position obtained for an untilted grid 2. (It has been assumed that θ and ϕ are small so that $\tan\theta = \theta$, etc.). Substituting into Eq. (1) gives an expression for the steering angle in the upper half of the geometry:

$$\theta_U = \theta_0 - [x - \phi\theta_0(x+X)]\left\{\frac{\Gamma}{4d_{2U}} - \frac{(1-0.2k)}{3d_{1U}} + \frac{d_{2U}}{9d_{1U}^2}\left[\frac{2}{\Gamma} - \frac{4(U^{1.5}-1)}{3\Gamma^2}\right](1-0.4k)\right\}. \tag{10}$$

Substituting for d_{1U} and d_{2U} and eliminating second-order terms of ϕ gives

$$\theta_U=\theta_0-\frac{x}{f_1}+\phi\left\{\begin{array}{l}\dfrac{(x+X)\theta_0}{f_1}+\dfrac{x(x+X)\Gamma}{4d_2^2}+\dfrac{x(x+X)(1-0.2k)}{3d_1^2}\\ +\dfrac{x(x+X)d_2}{9d_1^2}\left[\dfrac{2}{\Gamma}-\dfrac{4(U^{1.5}-1)}{3\Gamma^2}\right](1-0.4k)\left(\dfrac{1}{d_2}+\dfrac{2}{d_1}\right)\end{array}\right\}. \tag{11}$$

The first two terms of Eq. (10) represent the normal focusing action of the lens, while the third term represents the additional angular displacement due to the grid tilt. A similar expression is obtained for the lower half of the geometry, taking account of the sign convention, so that the steering angle of Eq. (2) is

$$\theta_s=\phi\left\{\begin{array}{l}\dfrac{(x+X)\theta_0}{f_1}+\dfrac{x(x+X)\Gamma}{4d_2^2}+\dfrac{x(x+X)(1-0.2k)}{3d_1^2}\\ +\dfrac{x(x+X)d_2H}{9d_1^2\left(\dfrac{1}{d_2}+\dfrac{2}{d_1}\right)}\end{array}\right\}, \tag{12}$$

where

$$H=\left[\frac{2}{\Gamma}-\frac{4(U^{1.5}-1)}{3\Gamma^2}\right](1-0.4k).$$

B. Rotation at the third grid

Figure 2 shows a generalized geometry for the case where grid 3 is tilted with respect to the other elements. In this case, the transport of the beam through the lens at grid 2 must be considered to obtain the relevant angular and radial positions at grid 3. Clearly, both the lenses at grids 2 and 3 are affected by the tilt. (Note that the analysis of the second grid tilt only considers the effect up to and including the lens at this grid).

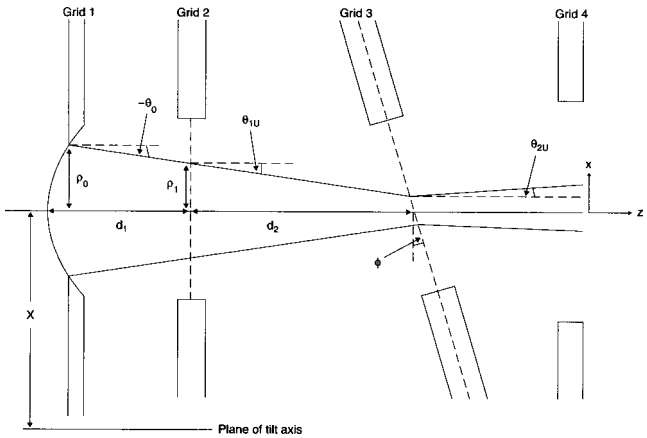

FIG. 2. Geometry for the case of tilted grid 3 in a tetrode accelerator. The electrodes are labeled sequentially from the left- and to the right-hand side.

The equations for the steering at grid 3 are identical to those for grid 2 except that θ_0 is replaced by θ_1, the angle of the beam leaving grid 2 and ρ_1, the beam radius at the second grid, replaces ρ_0. Thus,

$$\theta_{2U}=\theta_{1U}-\frac{x_U}{f_{2U}}, \tag{13}$$

where x_U is now the vertical position from the aperture axis at grid 3 in the upper half of the geometry and f_{2U} is the focal length of the lens at grid 3 at x_U. As before $x_U=x-\phi\theta_1(x+X)$ and $d_{2U}=d_2-(x_U+X)\phi$. The focal length of the lens at grid 3 is given by:[9]

$$\frac{1}{f_2}=-\frac{\Gamma}{4d_2U}-\frac{d_2}{9d_1^2U}\left[\frac{2U^{0.5}}{\Gamma}-\frac{4(U^{1.5}-1)}{3\Gamma^2}\right](1-0.4k). \tag{14}$$

Substituting for d_{2U} and x_U in Eqs. (13) and (15) gives

$$\theta_{2U}=\theta_{1U}-[x-\phi\theta_1(x+X)]\left\{-\frac{\Gamma}{4Ud_2}\left[1+\frac{\phi(x+X)}{d_2}\right]-\frac{d_2G}{9d_1^2U}\left[1-\frac{\phi(x+X)}{d_2}\right]\right\}, \tag{15}$$

where

$$G=\left[\frac{2U^{0.5}}{\Gamma}-\frac{4(U^{1.5}-1)}{3\Gamma^2}\right](1-0.4k).$$

The angle θ_{1U} is obtained from Eqs. (1) and (3) with $d_{1U}=d_1$ and $d_{2U}=d_2-(x_U+X)\phi$ and substitution into Eq. (14), while adopting the same approximation of ignoring second-order terms of ϕ, gives

$$\theta_{2U}=\tan\theta_0-\frac{\rho_0(1+k)}{f_1}-\frac{x}{f_2}+\phi\left\{\frac{x(x+X)\Gamma}{4Ud_2^2}-\frac{x(x+X)G}{9Ud_1^2}\right\}+\phi\rho_0(1+k)\left\{\frac{(x+X)H}{9d_1^2}-\frac{(x+X)\Gamma}{4d_2^2}\right\}+\phi\theta_1\left\{\frac{(x+X)G}{9Ud_1^2}-\frac{(x+X)\Gamma}{4Ud_2}\right\}, \tag{16}$$

where f_1 and f_2 refer to the focal lengths for untilted grids. Thus, the total steering angle, θ_s, is

TABLE I. Accelerator dimensions for the numerical calculation.

Aperture	Diameter (mm)	Electrode spacing	Length (mm)
Grid 1 (a_1)	12	G1-G2(d_1)	5.12
Grid 2 (a_2)	13	G2-G3(d_2)	10.83
Grid 3 (a_3)	10		

$$\theta_s=\phi\left\{\frac{x(x+X)\Gamma}{4Ud_2^2}-\frac{x(x+X)G}{9d_1^2U}+\rho_0(1+k)\left[\frac{(x+X)H}{9d_1^2}-\frac{(x+X)\Gamma}{4d_2^2}\right]+\theta_1\left[\frac{(x+X)G}{9d_1^2U}-\frac{(x+X)\Gamma}{4Ud_2}\right]\right\}. \tag{17}$$

C. Effect on beam perveance

The variation in the gap length due to a tilted grid will cause a variation of perveance across the grid. This can be briefly examined by averaging the Child–Langmuir equation across the grid, between the limits $-w_1$ and $+w_2$, where w is the distance from the tilt axis. The Child–Langmuir equation gives

$$P(d)=\frac{K}{d^2}, \tag{18}$$

where $K=(4\pi\rho^2\varepsilon_0/9)\sqrt{2e/m}$. For the constant d (i.e., no tilt), averaging over the grid gives

$$P_0=\int_{-w_1}^{+w_2}\frac{K}{d_0^2}dw\Big/\int_{-w_1}^{+w_2}dw=\frac{K}{d_0^2}. \tag{19}$$

In the case of a tilted grid, the distance d is given by $d=d_0-w\phi$ and the average is

$$P=\int_{-w_1}^{+w_2}\frac{K}{d_0^2}\left(1+\frac{2w\phi}{d_0}\right)dw\Big/\int_{-w_1}^{+w_2}dw$$

$$=\frac{K}{d_0^2}\left[1+\frac{\phi}{d_0}(w_2-w_1)\right], \tag{20}$$

where, as before, terms in ϕ^2 have been dropped. Thus, the perveance ratio of the tilted and untilted cases is

$$\frac{P}{P_0}=1+(w_2-w_1)\frac{\phi}{d_0}. \tag{21}$$

Equation (21) allows the approximate position of the tilt to be determined if ϕ is known and vice versa. It also shows that when $w_2=w_1$, the perveance is unaffected as the shortened and lengthened gaps cancel. (This assumes a perfectly uniform plasma density across the grid. Note also that there is a third-order term in the integration which is not zero when $w_1=w_2$, however, it is much less than unity for reasonable values of ϕ). If the tilt axis is positioned such that $w_2>w_1$, then $P>P_0$, i.e., the perveance at minimum beam dimensions will be increased.

The perveance analysis can be used to obtain a unique value for θ_s if ϕ is known. If the full span of apertures in the grid is L and the distance of the tilt axis from the edge of the aperture array is ζ, then setting $w_2=L-\zeta$ and $w_1=\zeta$ in Eq. (21) gives

$$\zeta=\frac{1}{2}\left[L-\left(\frac{P}{P_0}-1\right)\frac{d_0}{\phi}\right], \tag{22}$$

from which X can be obtained and substituted into Eqs. (12) and/or (17). (Note that X and ζ are not the same but are related by a shift of origin from the tilt axis to the edge of the aperture array.)

III. NUMERICAL EXAMPLES

Equations (12) and (17) were used to calculate typical steering angles that might be obtained from a tilted grid for the high current tetrode PINI. The values for the geometry parameters are given in Table I. To obtain the values of d_1 and d_2, it is assumed that the plane of the electrostatic lens

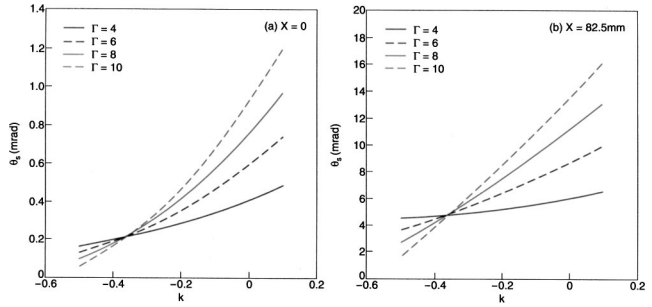

FIG. 3. Steering angles for a rotation of grid 2 (a) for an aperture on the axis of rotation, $X=0$ and (b) for an aperture at the edge of the PINI grid, $X=82.5$ mm. The angles are plotted as a function of the variable k which describes the curvature of the plasma boundary as a function of beam perveance. The curves are parametrized by the voltage ratio Γ.

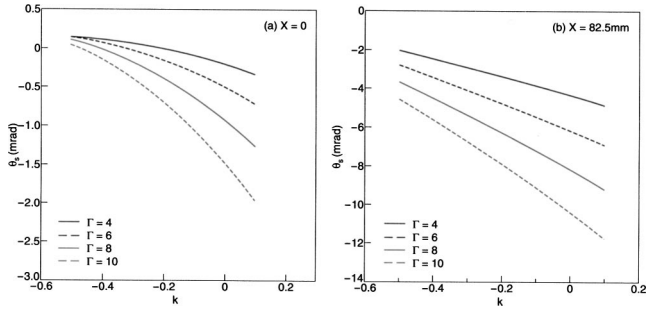

FIG. 4. Steering angles for a rotation of grid 3 (a) for an aperture on the axis of rotation, $X=0$ and (b) for an aperture at the edge of the PINI grid, $X=82.5$ mm. The angles are plotted as a function of the variable k which describes the curvature of the plasma boundary as a function of beam perveance. The curves are parametrized by the voltage ratio Γ.

TABLE II. Power loading on beamline elements as percentage of beam power (IxV) at perveance match for perfect PINI (16AT3) and "suspect" PINI 13ATGS.

PINI	Grid 2 (%IxV)	Grid 3 (%IxV)	Grid 4 + neutralizer (%IxV)	Box scraper left-hand size(%IxV)	Box scraper right-hand side (%IxV)	Perveance (μP)	Beam voltage (kV)
16AT3	0.27	0.39	0.73	0.92	1.22	1.6778	72.8
13ATGS	0.42	0.64	2.18	0.48	0.36	1.839	58.4

at grid 2 lies at the center of that grid and that the electrostatic field penetrates a distance $2a_3/3$ into the aperture of grid 3, an empirically derived value.[9]

A correction factor, z, modifies the gap lengths to account for the curvature of the equipotential surface at the midplane of G2. It is obtained by solving the polynomial equation[9]

$$z=\left\{\frac{\Gamma}{[(d_2/d_1)^2+(a_3/d_1)^2]^{0.5}}-1\right\}\left(\frac{a_2}{6}-\frac{z^2}{4a}+\frac{z^4}{16a^3}\right). \tag{23}$$

Values of the steering angle, θ_s for rotation of grids 2 and 3 were calculated for two cases: (i) for an aperture located on the axis of tilt ($X=0$) and (ii) for an aperture located at $X=82.5$ mm from the tilt axis. The latter case corresponds to an aperture at the edge of the PINI grid when the tilt axis lies in the vertical plane through the center of the grid. Assuming a tilt angle of $\phi=1$ mrad, the value of the steering angle was calculated as a function of the parameter k for four typical values of Γ in each case and the results are shown in Figs. 3 and 4.

Figure 3 shows the results for a tilted grid 2. As might be expected, the aperture at the edge of the grid shows stronger steering than that on axis, with steering angles up to 500% of the tilt angle for typical values of k and Γ. Note also that θ_s is positive (i.e., away from the beam axis) for positive ϕ as defined in Fig. 1. For negative values of ϕ, the direction of steering is reversed.

Figure 4 shows the equivalent results for the case of a tilted grid 3. In this case, the direction of the steering angle depends upon k and the position of the aperture with respect to the tilt axis, although for most practical applications, the steering will be toward the beam axis for positive ϕ as defined. Again, for negative values of ϕ, the direction of steering is reversed. Thus the effect of steering by a rotated grid can either enhance or detract from intended off set aperture steering, depending upon the geometry of the rotation and the operational parameters of the injector.

IV. APPLICATION TO PINI 13ATGS

As indicated in Sec. I, the motivation for this work was the observation of poor beam optics and anomalous perveance of the PINI 13ATGS. Table II compares the power loadings (as a percentage of extracted ion beam power) for 13ATGS and a "perfect" PINI 16AT3. The measurements are made on the accelerator grids and two box scraper elements situated 5.78 m downstream from the PINI. (The box scraper simulates the position of the Neutral Injector Box exit beam scrapers on the actual JET Injection System).[3] The power loading on the grids and neutralizer are considerably greater for 13ATGS than for 16AT3, but reduced on the box scraper; this is consistent with significant beam loss inside the accelerator. In addition, the distribution of power between the left- and the right-hand side box scraper elements is reversed, indicating a gross steering of the beam to the left-hand side (viewed from the PINI source) by 13ATGS. Observation of the intercept marks on grid 3 implied that the beamlets at the edge of the grid were displaced away from the beamlet axis, consistent with the model for a rotation of grid 2 in the horizontal plane. Approximately 1–2 mm of beam was incident on the grid and as the beam approximately fills the grid 3 aperture, this implies that $\theta_s \approx 150$ mrad.

The calculations of Sec. II can be applied to the test results for the PINI 13ATGS. The PINIs are operated with a fixed value of $\Gamma=9$, thus the data of Table II correspond to $V_1=5.84$ kV and $V_2=52.56$ kV; the values of d_1, d_2, etc., are those in Table I. The tilt axis must lie within the opposite grid half to the aperture under consideration because of the perveance condition $P>P_0$. From the beam perveance at a minimum beam radius (given in Table II) and the plain diode perveance calculated from the PINI geometry, the effective value of k, averaged across the grid, is estimated to be $k=-0.3$.

The tilt angle, ϕ, is limited by the maximum displacement at the grid edge consistent with electrical isolation. In

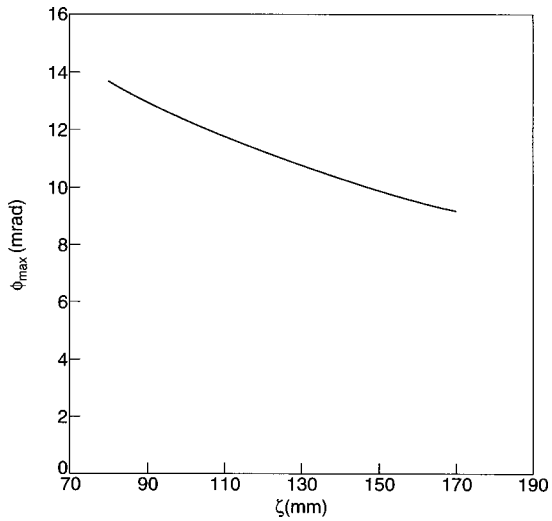

FIG. 5. The limiting value of rotation angle, ϕ, imposed by electrical isolation of the second grid as a function of the distance from the extremity of the aperture array to the rotational axis.

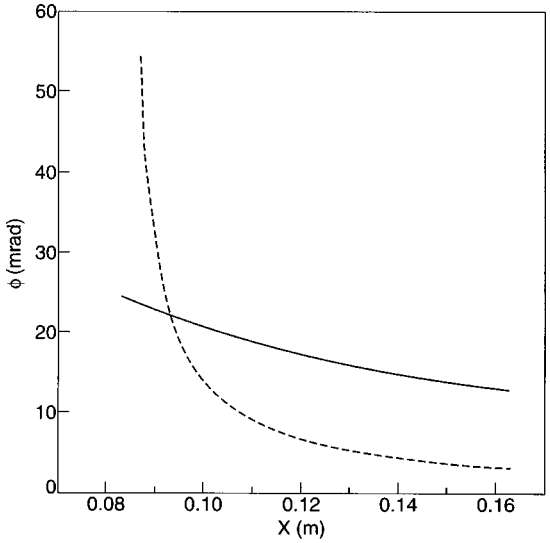

FIG. 6. Graphical simultaneous solution [of Eqs. (12) (—) and (22) (---)], for a beamlet at the extremity of the aperture array, to obtain ϕ and X for PINI 13ATGS. The point of intersection gives $X=93$ mm and $\phi=22$ mrad.

the PINI, this maximum displacement is 2.5 mm and the limiting tilt angle as a function of ζ is shown in Fig. 5. Equations (12) and (22) can now be solved simultaneously to give X and ϕ, using the relationship

$$X=\Lambda_n-\zeta, \tag{24}$$

where Λ_n is the position of the aperture with respect to the opposite edge of the array. Figure 6 shows the graphical solution for $\Lambda_n=165$ mm. The corresponding values of X and ϕ are $X=93$ mm and $\phi=22$ mrad. Unfortunately this tilt angle lies outside the range of allowed values, although it is of the correct order and given the simplicity of the model it would be surprising if an exact correlation was obtained.

V. DISCUSSION

A simple optics model of the effect of tilted grids has shown that considerable steering angles can be generated for quite modest tilt angles. In the parameter space in which the PINIs generally operate, steering angles of the order 3 mrad per mrad of tilt are possible for both grid 2 and grid 3 cases. The effect of a tilt on beam perveance has also been considered and shown to be consistent with the results obtained from 13ATGS.

The article treats each grid independently and a combination of grid tilts and offset aperture steering is beyond this method of analysis. However, computational modeling could treat a combination of these effects relatively easily.

In view of the results, the FARO-Arm® technique for positional measurements of the accelerator grids has been modified to enable grid tilt to be detected on assembly of the PINI, with the resulting elimination of the delivery of poorly aligned injectors to the neutral beam test bed.[8]

ACKNOWLEDGMENT

The author would like to thank Dr. A. J. T. Holmes, Marcham Scientific, for discussions during this work.

[1] T. C. Jernigan, R. C. Davies, O. B. Morgan, D. E. Schlechter, L. D. Stewart, W. L. Stirling, and R. E. Wright, Proceedings of the Symposium on Ion Sources and Formation of Ion Beams, Berkeley LBL 3399, VI-9-1 (1974).
[2] T. S. Green and J. R. Coupland, *Ion Beam Deflection in Extraction Electrodes*, Culham Report CLM-P410, UKAEA (1974).
[3] G. Duesing *et al.*, Fusion Technol. **11**, 163 (1987).
[4] E. Surrey, D. Ciric, D. J. Godden, and B. Crowley, Proceedings of the 19th IEEE/NPSS Symposium on Fusion Engineering, Atlantic City, NJ (2002), p. 64.
[5] J. R. Conrad, Rev. Sci. Instrum. **51**, 418 (1980).
[6] J. H. Whealton, R. W. McGaffey, and E. F. Jaeger, Report ORNL-TM-6944, Oak Ridge NL (1979).
[7] M. Tartz, E. Hartmann, R. Deltschew, and H. Neumann, Rev. Sci. Instrum. **73**, 928 (2002).
[8] D. Ciric, J. Milnes, and E. Surrey, Proceedings of the 19th IEEE/NPSS Symposium on Fusion Engineering, Atlantic City, NJ (2002), p. 56.
[9] A. J. T. Holmes and E. Thompson, Rev. Sci. Instrum. **52**, 172 (1981).
[10] J. H. Whealton, Rev. Sci. Instrum. **48**, 1428 (1977).